Visual Neuroscience (1989), 2, 41–55. Printed in the USA.

Role of inhibition in the specification of orientation selectivity of cells in the cat striate cortex

A. B. BONDS

Department of Electrical Engineering, Vanderbilt University, Nashville

(RECEIVED February 4, 1988; ACCEPTED June 28, 1988)

Abstract

Mechanisms supporting orientation selectivity of cat striate cortical cells were studied by stimulation with two superimposed sine-wave gratings of different orientations. One grating (base) generated a discharge of known amplitude which could be modified by the second grating (mask). Masks presented at nonoptimal orientations usually reduced the base-generated response, but the degree of reduction varied widely between cells. Cells with narrow orientation tuning tended to be more susceptible to mask presence than broadly tuned cells; similarly, simple cells generally showed more response reduction than did complex cells.

The base and mask stimuli were drifted at different temporal frequencies which, in simple cells, permitted the identification of individual response components from each stimulus. This revealed that the reduction of the base response by the mask usually did not vary regularly with mask orientation, although response facilitation from the mask was orientation selective. In some sharply tuned simple cells, response reduction had clear local maxima near the limits of the cell's orientation-tuning function.

Response reduction resulted from a nearly pure rightward shift of the response *versus* log contrast function. The lowest mask contrast yielding reduction was within 0.1–0.3 log unit of the lowest contrast effective for excitation.

The temporal-frequency bandpass of the response-reduction mechanism resembled that of most cortical cells. The spatial-frequency bandpass was much broader than is typical for single cortical cells, spanning essentially the entire visual range of the cat.

These findings are compatible with a model in which weak intrinsic orientation-selective excitation is enhanced in two stages: (1) control of threshold by nonorientation-selective inhibition that is continuously dependent on stimulus contrast; and (2) in the more narrowly tuned cells, orientation-selective inhibition that has local maxima serving to increase the slope of the orientation-tuning function.

Keywords: Visual cortex, Visual receptive fields, Inhibition, Orientation selectivity

Introduction

The response amplitude of cells in the striate cortex typically depends on the orientation of moving, one-dimensional stimuli (see Orban, 1984 for review). Two general models have been proposed to account for cortical orientation selectivity, one relying principally on excitation, the other on a combination of excitation and inhibition. Hubel and Wiesel (1962) hypothesized that the receptive field of a simple cell is constructed from the convergence of excitatory afferent fibers from lateral geniculate nucleus (LGN) cells whose receptive fields formed a roughly linear array. Bars oriented in parallel with these arrays would provide maximum excitation, while orthogonally oriented bars would excite minimally as well as invoke inhibition from LGN receptive-field surrounds. This hypothesis is attractive in its simplicity, but is insufficient by itself. A linear array is unlikely to be adequate to support tuning as narrow as 5 deg, which is seen in some cells (Orban, 1984). Even though LGN cells have been reported to show some innate orientation preference (Vidyasagar & Urbas, 1982; Soodak et al., 1987), they nonetheless respond vigorously to stimuli presented at all orientations. Suppression of some kind is required to account for the failure of most cortical cells to respond when stimulated by bars with orientations orthogonal to the optimal axis (Hubel & Wiesel, 1962).

The alternate model proposes that excitation of cortical cells is influenced minimally by stimulus orientation, and that selectivity is shaped instead by intracortical inhibition. The inhibition is itself considered to be orientation selective and is tuned in opposition to a cell's excitatory tuning function so that the inhibition would be greatest for orthogonal stimuli (e.g. Bishop et al., 1973; Creutzfeldt et al., 1974*b*; Sillito, 1975; Nelson & Frost, 1978). This hypothesis was first suggested by the observation that an artificially elevated maintained discharge could be

Reprint requests to: A.B. Bonds, Department of Electrical Engineering, P. O. Box 1824B, Vanderbilt University, Nashville, TN 37235, USA.

suppressed by presentation of a stimulus at the orthogonal orientation (Bishop et al., 1973; Sillito, 1979; Heggelund, 1981*a*,*b*; Morrone et al., 1982). Support for this hypothesis also comes from work with agents that block gamma-aminobutyric acid (GABA), a neurotransmitter that mediates intracortical inhibition. Iontophoretic application of the GABA-blocker bicuculline has been reported to reduce or eliminate orientation selectivity in both simple and complex cells, although not all cells were affected in this way (Sillito, 1977, 1979; Tsumoto et al., 1979; Sillito et al., 1980).

The work presented here is intended to define more completely the nature of intracortical inhibition and its role in controlling the spatial organization of the cortical receptive field. The experimental approach is an extension of the double-stimulus paradigm introduced by Bishop et al. (1973) in which one stimulus is used to elevate the discharge of a cell, providing a background against which the suppressive or facilitatory impact of a second stimulus can be seen. This has the advantage of avoiding complex pharmacological interactions that may arise from iontophoresis of neurotransmitter blocking agents. Here, one sine-wave grating pattern (the base) is configured at the orientation and spatial frequency that is optimal for driving the cell. A second grating (the mask) is electronically superimposed on the first. Variation of the spatial characteristics of the mask reveals facilitatory or suppressive influences on the cell under study as reflected by modification of the base-induced response.

Methods

Surgical preparation

Studies were conducted on 18 adult (2.5–4.0 kg) cats. Anesthesia was induced with 5% Fluothane (halothane) in O_2 and a forelimb vein was cannulated for subsequent infusion of anesthetic and paralyzing agents. During the remainder of surgery, the gas was discontinued and 2.5% sodium thiamylal was infused as required. A tracheal cannula was inserted and the cat was mounted in a stereotaxic apparatus. The scalp was reflected on the midline and electrodes were inserted over the lateral suprasylvian gyri for the monitoring of generalized brain activity. A 1 mm × 3 mm hole was drilled at Horsley-Clarke coordinates P4-L2, directly over the *area centralis* representation in area 17. The dura was incised and after positioning of the electrode over an area free of surface vessels the hole was covered with agar mixed in mammalian Ringer's solution. Melted Tackiwax (Cenco, Chicago, IL) was then poured over the agar to provide an effective hydraulic seal.

Recording conditions

In order to suppress eye movements, the cats were paralyzed with gallamine triethiodide (Flaxedil) at 10 mg/kg-h and ventilated with a mixture of N_2O:O_2:CO_2 (75:23.5:1.5) at 30 min^{-1} with a stroke volume sufficient to hold expired pCO_2 at 3.9%. The infusate also included 1 mg/kg-h Surital to maintain effective anesthesia (Hammond, 1978) as well as lactated Ringer's solution. Monitoring of the EEG and EKG provided general indications of the animal's state of anesthesia and health. Rectal temperature was maintained at 37.5°C with a servo-controlled heat pad. Eyelids were retracted and the natural pupils were dilated by instillation of 10% phenylephrine HCl and 1% atropine sulfate in the conjunctival sacs. Contact lenses with 4-mm-diam artificial pupils were fitted to the nearest 0.5-m base curve radius and auxiliary lenses were added as dictated by direct ophthalmoscopy to render the retinae conjugate with the viewing screen 57 cm distant. Retinal landmarks (optic disk and *area centralis*) were projected onto the plotting screen with a reversible ophthalmoscope. All recorded cells had receptive fields located within 5 deg of the *area centralis*. Action potentials were recorded with tungsten-in-glass microelectrodes (Levick, 1972) with uninsulated tips 18–20 μm long and 2 μm wide at the shoulder.

Stimulation

The primary stimulator was a CRT display (Tektronix 608; mean luminance 110 cd/m^2, P31 phosphor) with a 10-deg circular field. The display was compensated for linear modulation up to 75% contrast. Sine-wave gratings were generated with a microprocessor-based pattern generator similar in concept to that described by Milkman et al. (1978). The pattern generator supported independent control of the spatial frequency and phase, contrast, orientation, and drift rate of up to four patterns. Multiple patterns were superimposed by alternating frames of each pattern at a rate of 256/s; with two patterns, each was presented at 128/s. All stimulation was monocular.

Data acquisition and processing

The primary data analysis tool was construction of 2-s, 128 bin/s poststimulus time histograms. To reduce artifact from the inherent nonstationarity of visual cortex, the interleaved histogram technique of Henry et al. (1973) with randomization was used exclusively. Each experiment was constructed with measurements parametric on one or two variables. A stimulus set was specified comprising each measuring condition as well as a null condition (uniform field at the mean luminance of the gratings) to assess the maintained discharge. Each element in the stimulus set was presented once, in random order with 1 s of mean luminance between each presentation, until the set was exhausted. Presentation of the set was then repeated in a different random order until each stimulus condition had been tested ten times. With 4-s presentation periods, results are based on 40 s of averaging for each condition. The number of impulses per presentation was tracked to permit calculation of response variability.

Cell classification and response measurement

Receptive-field properties were first plotted by hand and cells were initially categorized as simple or complex according to the criteria of Hubel and Wiesel (1962). Cells with noticeable end-stopping were discarded, as that property would cause complications in these experiments. Final cell classification was based on responses to drifting sine-wave gratings. All simple cells, even the most spatially nonlinear, respond to moving gratings with a modulation of discharge rate in synchrony with the temporal frequency of drift, at least when the spatial frequency of the stimulus is near the cell's optimum. At all but the lowest spatial frequencies, complex cells respond with an increase in the mean firing rate without temporal modulation (e.g. Movshon et al., 1978*a*,*b*; DeValois & Tootell, 1983). Calculation of the modulation index (ratio of the fundamental response com-

ponent to the mean firing rate, or d.c. component; Movshon et al., 1978*a*) for each cell yielded a bimodal distribution. All cells with a modulation index greater than 1 corresponded to the simple class of Hubel and Wiesel, and those with a modulation index less than 1 corresponded to the complex class. Responses to single gratings were specified by the stronger response component, i.e. power at the fundamental frequency of stimulation for simple cells and d.c. power for complex cells. Because of temporal interactions between asynchronously drifting pairs of gratings, responses to these stimuli were usually expressed by the d.c. power component for all cells. Harmonic components were sometimes considered in defining the responses to double gratings, as indicated in the results. The maintained discharge rate, measured during an interval in which the screen was illuminated uniformly at the mean luminance of the gratings, was expressed by the appropriate response component (harmonic fundamental for simple cells, d.c. for complex cells) and is indicated by a star near the ordinate of each figure. Whenever practical, measurements were made at several contrasts both to observe the effect of alterations of experimental parameters on the contrast-response function and to assure the consistency of the result.

Interpretation of dual-grating results

In these experiments, the first grating, the base, was used simply to drive the cell under study to a moderate level of activity so that any influence on the firing level resulting from the presence of the second grating, the mask, could be clearly seen. In order to maximize the dynamic range of mask-induced response modification, the contrast of the base was set to a value that produced a response that was about half of highest firing rate found by a separate response *versus* log contrast measurement. The base was always presented at the best orientation and spatial frequency for the cell, which was determined by independent quantitative measures. Use of an optimal base stimulus was intended to minimize involvement of spatially selective inhibitory mechanisms. As will be seen, this strategy was probably not important.

The impact of the mask on the base-generated activity can most easily be understood by considering that each stimulus is presented in alternate frames by the stimulator. If the mask were not present, then the base would alternate with a frame of uniform luminance, which would yield an *effective* base contrast of half of its nominal contrast. For this reason, every experiment that used two gratings also included an interleaved control measurement of the response to the base at half its nominal contrast; this response level is indicated by a horizontal dotted line in all figures. Facilitation by the mask elevated the discharge above this level; mask-induced suppression reduced the discharge below this level.

Michelson contrast, which defines contrast on the basis of maximum and minimum luminances, will not yield a consistent representation of the amount of luminance modulation when two dissimilar gratings are superimposed. Maximum and minimum luminances will correspond to the signed algebraic sum of the maximum and minimum luminances of each of the two gratings, which would predict that combined contrast was the simple summation of the Michelson contrasts. However, destructive interference between dissimilar gratings will reduce the contrast energy in the field. If contrast is defined as the standard deviation of luminance from the mean integrated over the field, by Parseval's theorem the contrast of any two superimposed gratings that differ spatially will be 0.707 times the sum of their individual contrasts. For this reason, the response, e.g. to two asynchronously drifted (but otherwise identical) gratings, is less than that to a single grating of a contrast that is the sum of the two. When double gratings are used here contrast will be described by stating the *effective contrast* (e.c.) of each constituent grating, which would be the Michelson contrast of that grating presented in alternation with a field of uniform mean luminance. The highest possible effective contrast of each grating is 50%, since each is presented only half of the time.

Results

Verification of the approach

Impact of interference

When the activity generated by the base grating is reduced in the presence of a superimposed mask grating, the claim that this suppression results from synaptic inhibition of the recorded cell by the mask is only valid if the reduction of response does not result from the reduction of excitation from the base, which could occur as a result of contrast cancellation between the gratings. Since the gratings are coextensive, destructive interference cannot be avoided. Two superimposed gratings of different orientation produce a Moire pattern with local bands of zero contrast that are oriented normal to a bisection of the angle between the two gratings. If the drift rate of the gratings is identical, these bands are stationary, with their location depending on both the angle and relative phase between the two gratings. Response reduction found for a particular mask orientation could therefore result not from synaptic inhibition generated by the mask but from reduction of contrast covering the receptive field.

Control experiments were designed to test both the impact of these bands on responsiveness as well as the effectiveness of a strategy intended to minimize this impact. In the first experiment, a mask grating was superimposed on a base grating and oriented so as to reduce excitation. Both base and mask were presented at the spatial frequency that was best for the cell under study. The mask was drifted at the same rate as the base grating (2 Hz) so that the zero-contrast bars were stationary. The initial spatial phase of the mask was varied over a full cycle (12 phases at 30 deg intervals). Every location in the stimulus field was therefore covered by a zero-contrast bar for at least one of these conditions. Results are shown in Fig. 1; all conditions showed some degree of response suppression, since all response levels fell below the control level generated by the base grating alone (horizontal dotted line). Most simple cells (26 of 32) showed organized sensitivity to phase manipulation in varying degrees (Fig. 1B, solid line), indicating some influence of the zero-contrast bands and posing a clear problem in deciding whether response reduction is due to synaptic inhibition or interference. Responses of the remaining six simple cells were independent of relative phase (Fig. 1A), as were responses from all (18) complex cells tested this way (Fig. 1C, solid line).

In order to apply the double-grating test unambiguously to all cells, an alternate approach was developed. When the base and mask gratings drift at different rates, the zero-contrast interference bands themselves drift at the beat frequency between the base and mask drift rates. Contrast is periodically

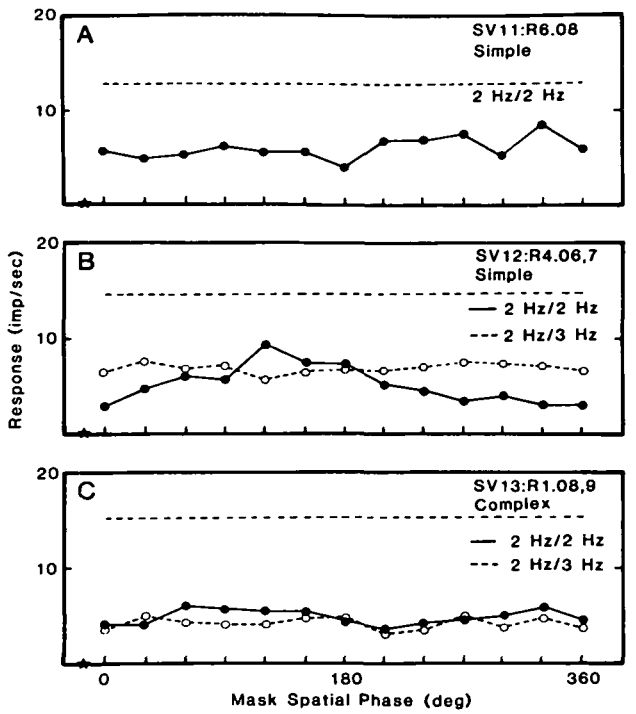

Fig. 1. Sensitivity to spatial phase of the interference pattern, tested by varying the initial spatial phase of the mask grating. The horizontal dotted line represents the control response to the base grating combined with a mask of zero contrast, and the maintained discharge level is represented by a star. A, 2-Hz response component from simple cell, with both base and mask drifted at 2 Hz, showing little organized phase sensitivity. Both gratings at 1.8 cycles/deg; base equivalent contrast (b.e.c.) 10%; mask equivalent contrast (m.e.c.) 20%. B, 2-Hz response component from simple cell showing phase sensitivity for 2-Hz mask (filled circles) and insensitivity for 3-Hz mask (open circles). Both gratings at 1.2 cycles/deg; b.e.c. 10%; m.e.c. 14%. C, Complex cell with no phase sensitivity for either 2-Hz (filled circles) or 3-Hz (open circles) mask. Both gratings at 1.1 cycles/deg; b.e.c. 14%, m.e.c. 14%. The cell codes marked on all figures represent the cat (e.g. SV11), cell (R6) and run number (.06), and allow identification of specific cells between figures.

reduced as the bands drift across the field, but is maintained over the majority of the measuring interval. The assumption is made that a *steady and strong* reduction of the base-induced response cannot be attributed solely to periodic reduction of contrast and must therefore involve synaptic inhibition. A simple cell that showed sensitivity to the interference bands was exposed to base and mask drifted at 2 Hz and 3 Hz, respectively. Response reduction remained strong and independent of the initial spatial phase of the mask (Fig. 1B, dotted line). Thus, although the interference bands cannot be eliminated, their effects on simple cells can be reduced through the use of dissimilar drift rates. This result was confirmed in all 12 simple cells examined this way. Even though complex cells did not exhibit phase sensitivity, the combination of a 2-Hz base and 3-Hz mask was equally effective in demonstrating suppression as a 2-Hz base and 2-Hz mask (Fig. 1C, dotted line). In all further experiments (except where noted), base and mask were drifted at 2 Hz and 3 Hz, respectively, to assure that the response reductions observed originated from neural, rather than optical interaction.

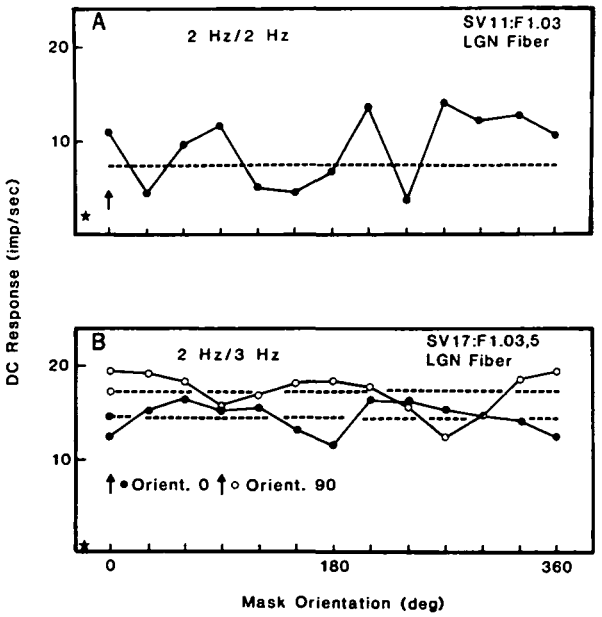

Fig. 2. Response of LGN fibers to crossed gratings of different orientations. Dotted line is response from base alone, star is maintained discharge. A, Drifting base and mask both at 2 Hz results in local minima due to interference. Spatial frequency of base and mask, 2 cycles/deg; base orientation is 0 deg (arrow); b.e.c. = m.e.c. = 14%. B: Drifting base and mask at 2 Hz and 3 Hz, respectively, results in smaller local minima seen only when gratings are parallel. Responses are from base orientations of 0 deg (filled circles) and 90 deg (open circles) as indicated by the arrows. Spatial frequency of base and mask, 0.6 cycles/deg; b.e.c. = m.e.c. = 20%.

Origin of suppression

In order to assign a specific site of action for the response suppression studied in these experiments, five LGN fibers coincidentally encountered while recording in striate cortex were tested by exposing their receptive fields to double grating patterns. If presentation of the mask grating to LGN receptive fields resulted in minimal response suppression, then it would be more likely that the suppression seen in cortical cells originated in the cortex. This would also support the demonstration above that grating interference was not of major importance. Both base and mask gratings were adjusted to the best spatial frequency for each LGN cell and the base was fixed at one orientation (usually horizontal) while the mask orientation was varied over 360 deg (30-deg intervals). Base and mask were drifted both at 2 Hz *versus* 2 Hz and 2 Hz *versus* 3 Hz. In the former case, the complications resulting from the stationarity of the interference bonds were obvious (Fig. 2A). Several (two or even three) clear response minima were seen as a function of mask orientation. However, in the 2-Hz *versus* 3-Hz condition, the excitation was generally uniform (Fig. 2B) across mask orientation. This is not to suggest that the cortical excitation was unaltered by the mask, but rather to say that, by the response measurement criteria used in these experiments, LGN responsiveness is more or less independent of mask orientation. The mask grating does cause a temporal redistribution of activity, but it is unlikely that this is primarily responsible for response reduction in cortical cells. Were this the case, LGN response peaks would have to be ideally distributed in time to

avoid temporal summation; this could not occur consistently over the broad range of mask orientations and receptive-field organizations for which the effect will be demonstrated.

All five of the LGN cells tested this way showed local minima for mask orientations parallel with the base. This could have resulted from total contrast cancellation when the asynchronously drifting (but otherwise identical) gratings periodically reached a relative phase of 180 deg. According to Parseval's Theorem, such cancellation results in lower "contrast power" integrated over time than is found for grating pairs differing in any spatial property (e.g. spatial frequency, orientation). These local contrast minima are not considered a problem, since the response reductions of interest in this work resulted from mask orientations that differ from that of the base.

General experimental procedures

The receptive field of each cell was mapped manually and classified followed by quantitative assessment, with grating stimuli, of the favored orientation and spatial frequency of the cell. The functions measured by varying the orientation or spatial frequency of a single grating in the customary way will be called *excitatory* tuning functions. A response *versus* contrast function was next measured with a single grating of optimal spatial frequency and orientation. Contrast for the base stimulus was selected from this curve by choosing a firing level that permitted observation of either an increment or decrement generated by the mask. The base contrast chosen usually fell between 5% and 20% effective contrast and in practice the lowest useful level was chosen to minimize interaction with the cortical contrast gain control (Ohzawa et al., 1985) or response saturation. The tuning functions derived by changing a parameter (e.g. orientation) of the mask grating will often be compared with excitatory tuning functions in which the same parameter was changed for a single grating. In general, the excitatory tuning functions were measured at a contrast equaling the sum of the effective contrasts of the base and mask grating pairs against which they are compared. In any event, contrast has little influence on the shape of the excitatory orientation-tuning function (Sclar & Freeman, 1982).

Orientation selectivity and suppression

Consider a simple experiment in which the orientation of the mask is varied, all other parameters remaining fixed. The resulting response pattern will be called the *inhibitory* orientation-tuning function. The two models for orientation selectivity, if strictly interpreted, predict two different experimental outcomes. The excitation evoked by the base grating is always assumed to remain constant, since the base is unchanged across all manipulations of the mask. In the excitatory model, the mask grating would add excitation that is orientation specific (either by fortuitous spatial arrangement of LGN receptive fields or from cortical cells that are themselves orientation selective) but would not modify the base-induced response when oriented outside the excitatory orientation band. The model based on spatially selective inhibition would similarly allow facilitation of the response by an optimally oriented mask, when the spatially selective inhibition is weakest. However, it would predict that a mask oriented outside the excitatory tuning band would reduce the base-induced response below the control level as a result of inhibition.

These alternatives were tested by varying mask orientation across the range of the excitatory orientation-tuning function in 52 cells. In initial experiments, only the d.c. response component (total spike count) was used to represent response amplitude for each experimental condition. Results are summarized in Fig. 3, which shows both excitatory and inhibitory orientation-tuning functions; the inhibitory functions were measured with identical base and mask contrasts. The strength and tuning of mask-induced response reduction varied greatly from cell to cell. Cells were grouped into three subjective categories corresponding to strong, moderate, and weak suppression when exposed to base and mask of equal contrast. Both simple and complex cells in the first category (Fig. 3A and B) showed a clear response reduction below the control level, often sufficient to block completely the base-induced excitation when the mask orientation was not optimal for the cell. The shape and bound-

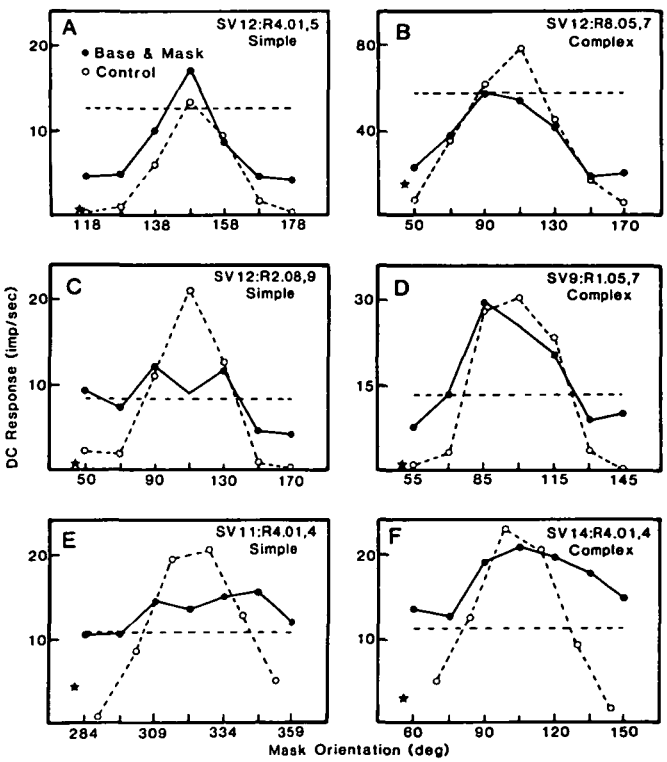

Fig. 3. Impact of mask orientation on d.c. response component of cortical cells. Base and mask are matched for spatial frequency and contrast and drift rates are 2 Hz (base) *versus* 3 Hz (mask). Base is always at the optimal orientation; excitatory tuning functions are represented by open circles, dotted lines; mask (inhibitory) tuning functions are represented by filled circles, solid lines. Horizontal dotted line is response from base alone; star is maintained discharge. Strong inhibition: A, Simple cell, spatial frequency 1.2 cycles/deg, e.c. 10%. B, Complex cell, s.f. 0.6 cycles/deg, e.c. 10%. Moderate inhibition: C, Simple cell, s.f. 0.4 cycles/deg, e.c. 14%. D, Complex cell, s.f. 1.4 cycles/deg, e.c. 10%. Weak inhibition: E, Simple cell, s.f. 0.8 cycles/deg, e.c. 10%. F, Complex cell, s.f. 0.4 cycles/deg, e.c. 14%. Note the different scales on the abscissae.

aries of inhibitory tuning functions of cells in this class often matched closely those of their excitatory tuning functions, suggesting that little but synaptic inhibition is required to define the excitatory bandwidth. Although this notion is in accord with the inhibitory models for orientation selectivity, it may be incorrect as will be discussed in the next section.

The cells that showed moderate suppression (Fig. 3C and D) gave clear reductions below the control response level when masks were oriented nonoptimally, but the pattern of these reductions did not match either in shape or amplitude the excitatory orientation-tuning function. These cells may therefore rely to some extent on synaptic inhibition to refine orientation selectivity, but require some other mechanism(s) for its fundamental specification. Cells in the third category (Fig. 3E and F) demonstrated some response facilitation when the mask neared the optimal orientation, but their responses never fell below the control level for any mask orientation, indicating minimal suppression by the mask grating at moderate contrasts. Note once again that the relative absence of suppression in these cases supports the idea that grating interference cannot be a major factor in response suppression. When cells in this category were exposed to mask gratings of higher (35–40%) effective contrast, all showed some response reduction to nonoptimally oriented gratings (e.g. Fig. 5B). This would suggest that differences in the responses to the mask gratings are a matter of the strength, rather than the absolute presence or absence of synaptic inhibition.

A summary of the distribution of cell types within these categories is given in Table 1. As also found by Morrone et al. (1982), simple cells more typically fall into the strong suppression category than do complex cells. This may be causally related to the tendency of simple cells to be more sharply tuned than complex cells, since those cells with the sharpest tuning were usually found to have strong suppression. Conversely, those cells with the broadest tuning tended to be complex and fell in the category of weakest suppression. Interestingly, two simple cells with fairly narrow tuning (16 deg and 19 deg half-width) were included in this latter category, suggesting that mechanisms other than inhibition can be important for orientation selectivity.

A mixed mechanism for orientation selectivity

To this point the two models for orientation selectivity, based on orientation-selective excitation or orientation-selective synaptic inhibition, have been considered as distinct. In view of the results presented above, it may be more realistic to think of a mechanism that is a combination of the two models in differing degrees that supports the broad spectrum of both orientation selectivity and mask-induced response suppression that is found between cells. Even this concept, however, may not be altogether correct. Since the base and mask were drifted at different temporal frequencies, in 14 simple cells that discharged synchronously with stimulation it was possible to separate, through Fourier analysis of the response, the relative contributions of base and mask to the overall response amplitude. This procedure requires a linear system for unambiguous resolution of response components. These cells are believed to be spatially linear (Movshon et al., 1978*a*) but do show response amplitude nonlinearities. Efforts were made to avoid saturation nonlinearities through use of low contrasts; nonetheless, these results must be accepted with some caution.

Since the excitation from the base remains independent of any manipulations of the mask stimulus, true orientation selectivity of inhibition would be reflected in orientation-dependent reduction of the base (2 Hz) response component. In many cases this is not found. Figure 4 shows responses of two simple cells as a function of mask-grating orientation. D.C. responses (total spike count) are shown in Fig. 4A and 4B; both cells would be categorized as showing strong suppression, and the shapes of the inhibitory tuning functions resemble those of the excitatory tuning functions. The next row (Fig. 4C and D) shows the 2-Hz response component as a function of mask orientation. Response reduction is a graded function of mask contrast, but the dependence on mask orientation is not the same as found for the d.c. response component. In Fig. 4C, response reduction is erratic, but essentially independent of mask orientation, indicating that whatever suppression that may be present *is not* orientation selective. In Fig. 4D, there is some consistent response reduction seen at the two most peripheral points of the tuning function, but the overall shape of the curve is much flatter than the excitatory tuning function (dotted line, Fig. 4B), indicating that even though the suppression is somewhat orientation selective, it is not likely to be the sole mechanism supporting the orientation selectivity of this cell. The dependence of the d.c. response components on mask orientation stems instead from the prominent 3-Hz (mask-induced) response component (Fig. 4E and F) that is (not surprisingly) shaped like the excitatory tuning function. The tuning of the 3-Hz response component is primarily due to orientation-selective excitation, since synaptic inhibition of the recorded cell would presumably affect both the 2-Hz and 3-Hz response components equally, and the 2-Hz curves are essentially flat in comparison with the 3-Hz curves. The absence of a 3-Hz response component when the cell is heavily suppressed also suggests that the suppression is not synchronized with the mask stimulus and therefore does not originate from a spatially coherent (e.g. single simple cell) mechanism.

The results of decomposing the response into separate components generated by base and mask demonstrates the caution which must be used in interpreting results involving response suppression. In earlier studies, suppression of an ongoing response by a stimulus that was not optimally (and was usually orthogonally) oriented was attributed to orientation-specific inhibition. It appears instead that *any* stimulus, regardless of configuration, is likely to cause suppression, but that this suppression is hidden by the excitation generated when the stimulus is configured optimally. The suppression is nonetheless

Table 1. *The qualitative distribution of cells, by type, into categories of inhibition strength*

	Strong inhibition	Moderate inhibition	Weak inhibition
Simple	14/30 (47%)	12/30 (40%)	4/30 (13%)
Complex	5/20 (25%)	9/20 (45%)	6/20 (30%)
Unclassed	1/2 (50%)	1/2 (50%)	0
Average tuning width (HWHH)	13.8 deg	17.4 deg	22.7 deg

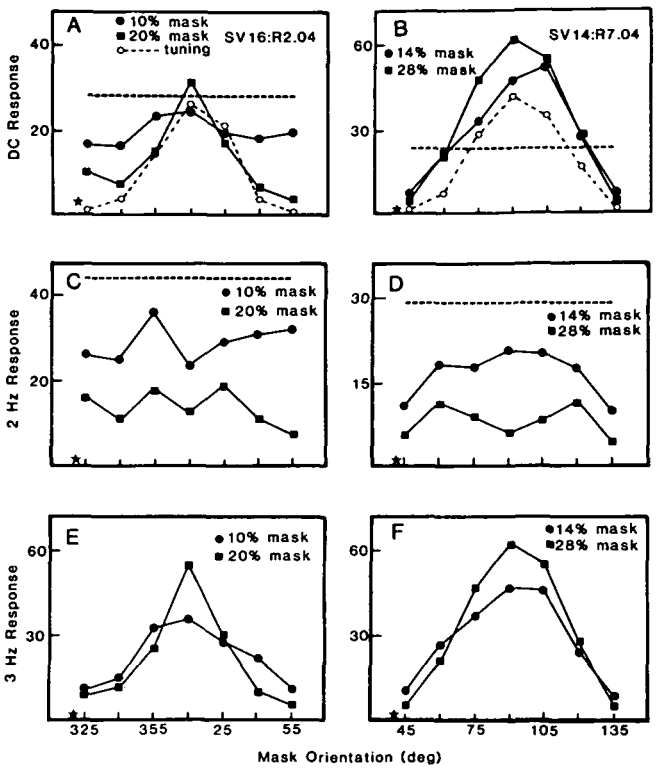

Fig. 4. Decomposition of simple cell responses. The 2-Hz response component represents stimulation from the base grating, the 3-Hz component represents that from the mask. The open circles, dotted lines in A and B represent the excitatory orientation tuning for each cell. Horizontal dotted line is response from base alone; star is maintained discharge. A,C,E are a measurement series on one cell. A, d.c. response for mask contrasts of 10% (filled circles) and 20% (squares), comparable with the information in the previous figure. C, 2-Hz response component at the same contrasts, showing inhibition that is not particularly organized with respect to mask orientation, but is strong and graded with contrast. E, 3-Hz response component that is clearly tuned to mask orientation. This tuning is essentially excitatory; inhibition would impose the same envelope on the 2-Hz response (C), which is not seen. Spatial frequency, 0.7 cycles/deg, b.e.c. 10%. B,D,F are similar observations on another cell. In this case, the 2-Hz component (D) is shaped somewhat by mask orientation, suggesting inhibitory peaks at 45 deg and 135 deg. The central dip seen at 28% mask contrast is likely due to response saturation; see text. Inhibition is still inadequate to account completely for the orientation tuning of the 3-Hz response (F). Spatial frequency, 0.4 cycles/deg; b.e.c. 7%.

present in the less-than-ideal summation of two excitatory response components.

Only three of the 14 cells that could be studied with response decomposition showed any organized sensitivity of the suppression to orientation (e.g. Fig. 4D), and in all of these cases the variation of suppression did not seem sufficient to support the overall tuning of the cell. Figure 4D also shows that when the mask contrast was increased (squares) the tuning of the 2-Hz response component was modified by a dip in the middle of the function. This can be explained by observing that the cell was being driven very strongly under this condition; the d.c. response exceeded 50 impulses/s, which is the point at which the response *versus* contrast function began to saturate. Use of a strongly saturating stimulus could lead to the conclusion that inhibition is particularly strong at the optimal orientation (Ferster, 1986), which is that condition most likely to saturate the cell's response. Under conditions of lower contrast, however (circles, Fig. 4D), the dip is not seen, indicating that optimally oriented stimuli would be less likely to generate inhibition as seen intracellularly if presented at lower contrasts. A dip in the middle of the 2-Hz function when mask contrasts drove responses into the saturation region was seen in four other cells (e.g. Fig. 5C).

The results exemplified in Fig. 4 therefore suggest, at least for simple cells, a compromise theory for the mechanisms supporting orientation selectivity. Excitation appears to be orientation dependent, as also found in the intracellular recordings of Ferster (1986). The behavior of response suppression also suggests synaptic inhibition, but unlike the usual models in which the inhibition is maximal for nonoptimal orientation, or the intracellular records of Ferster in which inhibition is maximal for the optimal orientation, most of the inhibition would be very broadly tuned with respect to the spatial qualities of the stimulus. In some cells, this "global" inhibition would be reinforced by a component of orientation-selective inhibition (e.g. Fig. 4D) that is studied more thoroughly in the next section.

Suppression outside the excitatory orientation bandwidth

In 24 cells, measurements were extended by positioning the mask at 12 orientations at 30-deg intervals and centered on the optimal orientation. Those cells with the broadest tuning and weakest suppression showed, in accord with the observation of Morrone et al. (1982), essentially uniform suppression across all orientations. The cell of Fig. 5A was simple, which allowed response decomposition as described above. The 2-Hz component is shown for mask contrasts of 20% (filled circles) and 40% (open circles). The former is nearly flat across mask orientation, while the latter shows a central dip presumably reflecting the effects of saturation (as in Fig. 4D). The d.c. response component of a weakly suppressive complex cell (Fig. 5B) shows no suppression until mask contrast is increased to 35% (open circles). Other cells with similarly broad excitatory orientation bandwidths could show much stronger suppression; in some cases increase of mask contrast could, for orthogonal mask orientations, reduce the firing level to a rate below that of the maintained discharge. A broad orientation bandwidth is therefore not necessarily a consequence of weak suppression.

The patterns of suppression of the 2-Hz response component of narrowly tuned simple cells (Fig. 5C and D) confirmed the existence of some degree of orientation selectivity similar to that shown in Fig. 4D. The filled circles (solid line), which indicate the 2-Hz response component, show in both cases local minima that indicate suppressive peaks near the orientations at which the excitatory orientation-tuning function approaches zero (the *limits* of the excitatory tuning function). Beyond these limits, the 2-Hz response rises, indicating decreased suppression. This is not totally inconsistent with the finding of Ferster (1986) that intracellularly measured inhibition is tuned like the excitatory tuning. The two schemes differ in that here suppression does not appear to be strongest at the optimal orientation. It is improbable that the strong excitation at the optimal orientation would itself prevent detection of inhibition at that orientation by the method of response decomposition; this would require an accelerating (rather than compressive) response non-

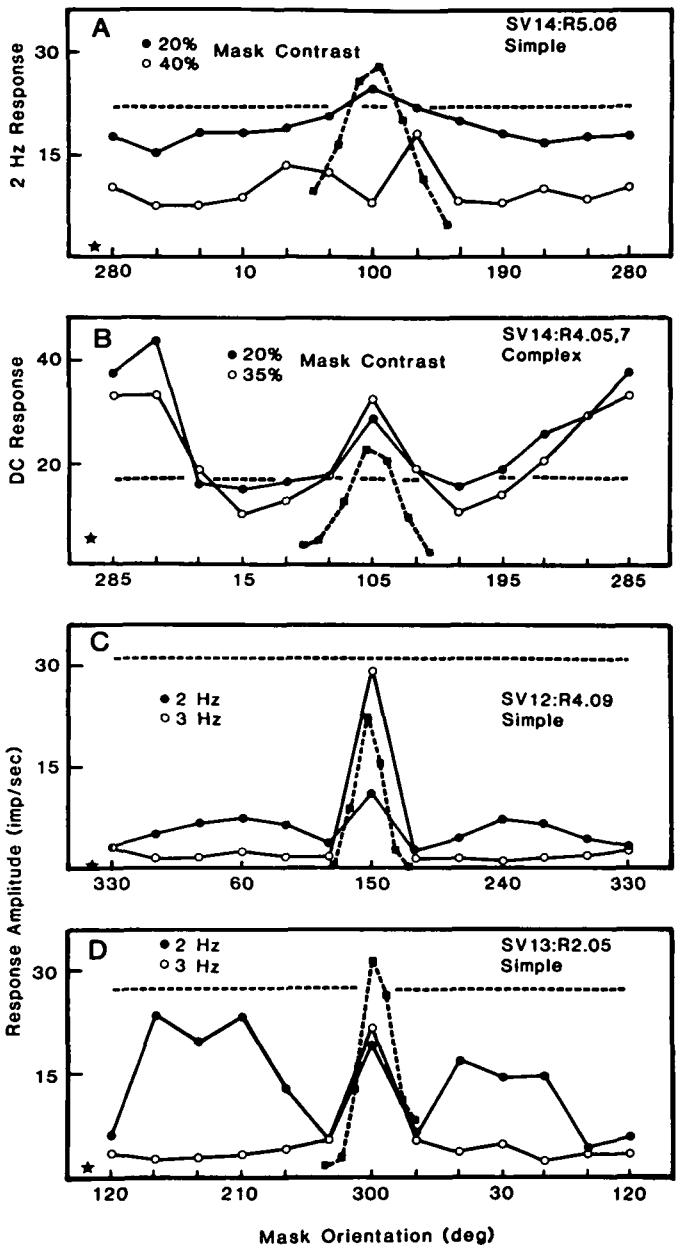

Fig. 5. Inhibition across all mask orientations. In each case the excitatory orientation-tuning function is outlined by dotted lines and filled squares. Horizontal dotted line is response from base alone; star is maintained discharge. A, 2-Hz response component from a broadly tuned simple cell; mask contrasts of 20% (filled circles) and 40% (open circles). Inhibition is clear but only weakly tuned for orientation. The central dip at 40% mask contrast is likely due to response saturation. Spatial frequency, 0.4 cycles/deg; b.e.c. 10%. B, A weakly inhibitory complex cell, d.c. response component. Inhibition is only seen for a mask contrast of 35%. Spatial frequency, 0.4 cycles/deg, b.e.c. 14%. C, Response decomposition for a sharply tuned simple cell. The 2-Hz (base; filled circles, solid line) response shows clear inhibitory maxima for mask orientations of 120 deg and 180 deg, corresponding to the limits of the excitatory tuning function. Inhibition is locally *minimal* at the orthogonal ("null") orientations. The 3-Hz (mask; open circles) response is more completely tuned than would be predicted from the inhibition revealed by the 2-Hz response. Spatial frequency, 1.2 cycles/deg, b.e.c. 10%, m.e.c. 20%. D, Similar example from another simple cell. Inhibition at the "null" orientation is very weak. Spatial frequency, 1.0 cycle/deg, b.e.c. 10%, m.e.c. 14%.

linearity. The characteristic "wing-like" structure resulting from peak suppression just at the limits of the excitatory tuning function enhances orientation discriminability by steepening the slopes of the tuning function. Both of these unidirectional cells also show strong suppression for motion in the wrong direction. Altogether, five simple cells (no complex cells; total sample of 24) with an average tuning of 11.7 deg half-width showed a similar notch at the limits of their excitatory tuning function. The common strategy of testing for inhibition with stimuli orthogonal to the optimal orientation (the so-called "null orientation") may not be very effective in such cases.

Dependence of response suppression on contrast

The contrast-response function of the suppressive mechanism was measured in 21 cells by orienting the mask so as to yield the maximum response reduction (usually at a limit of the excitatory tuning function; see above) and varying its contrast in 0.15 log unit intervals (Fig. 6). This procedure is not an absolute measure of the sensitivity or gain of suppression since the resulting curves depend on the amount of excitation provided by the base. The results do, however, permit some comparison between cells since this level of excitation was at about the same

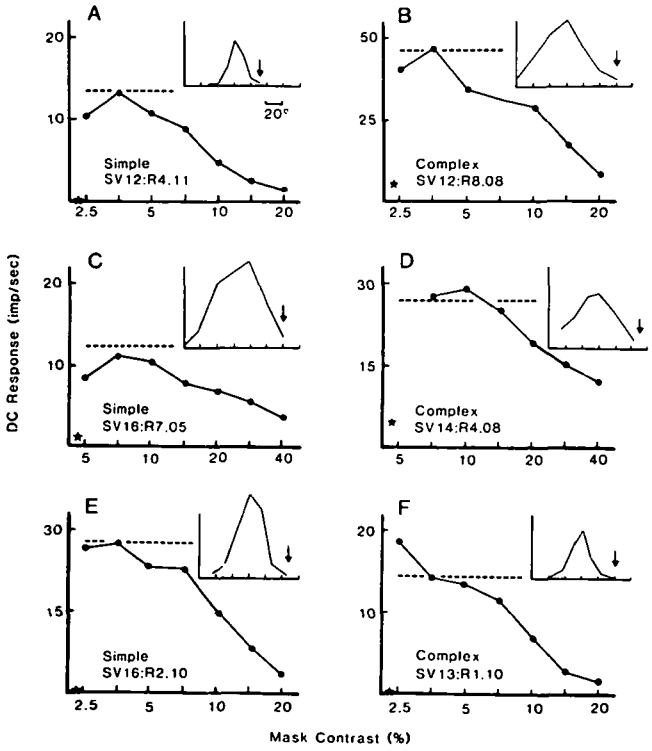

Fig. 6. Examples of the response dependence of the inhibitory mechanism on contrast. Masks were oriented at a limit of the excitatory tuning function (see arrows in insets). Horizontal dotted line is response from base alone; star is maintained discharge. There was some correlation between excitatory tuning width and strength of inhibition: narrowly tuned cells generally yielded response extinction at low mask contrasts (A,F), while broadly tuned cells did not (C,D). This was not always the case (B). A, Simple, spatial frequency 1.2 cycles/deg, b.e.c. 10%. B, Complex, s.f. 0.6, b.e.c. 10%. C, Simple, s.f. 1.0, b.e.c. 28%. D, Complex, s.f. 0.4, b.e.c. 14%. E, Simple, s.f. 0.7, b.e.c. 10%. F, Complex, s.f. 1.1, b.e.c. 14%.

relative point in the response range of each cell. The contrast at which the response monotonically departed from the control level was considered as the threshold for suppression. The average effective contrast at threshold was 7.2% and ranged from 3.5–28%, but this included many cells with only weak suppression. Those cells showing strong suppression (as defined above) generally had thresholds for suppression only about 0.1–0.3 log units above their excitatory thresholds. The (negative) slopes of the curves varied widely, reflecting the diversity in strength of suppression. Complete extinction of the base-induced response was found for mask contrasts as low as 14%; in six cells contrasts of 40% were insufficient to eliminate this response (Fig. 6C and D), but *all* cells tested this way showed some response reduction with increased mask contrast. When temporal segregation of response components was possible, no 3-Hz component ever exceeded the noise level. This is consistent with the absence of the 3-Hz component at nonoptimal mask orientations as described above and again indicates the asynchronous nature of the suppression.

In psychophysical masking studies, the presence of one pattern may make the detectability of a second pattern simultaneously presented more or less difficult. When the first grating is below its own contrast threshold, it enhances detectability of the second pattern; this process is usually attributed to statistical summation. When the first grating is above threshold, it reduces detectability of the second pattern; this is usually attributed to a compressive nonlinearity in a single spatial channel caused by added excitation (Legge & Foley, 1980). A physiological correlate of masking behavior was observed in most (14 of 21) of the experiments described above. As mask contrast was increased, the response *increased*—corresponding to subthreshold summation—before a decline (Fig. 6A-D). In most of the other cases, the decline of responsiveness was monotonic with mask contrast (Fig. 6F); since lower mask contrasts were not presented, subthreshold summation cannot be ruled out even in these cases. The clear and monotonic response suppression resulting from higher mask contrasts could, in a sense, mimic a compressive nonlinearity. However, the decrease in response elicited by the base grating is not a consequence of an increase in the overall activity of the cell, as would be predicted by the nonlinear transducer hypothesis. This would suggest that inhibition across spatial channels is a more likely substrate for suprathreshold masking.

Impact of suppression on the contrast-response function

This study assessed the effect of the mask grating on the response function measured by varying the contrast of the base grating. As in the previous exercise, the mask was situated at an orientation likely to cause suppression, but its contrast was fixed while measurements were made by varying the contrast of the base; this process was repeated at different mask contrasts. Figure 7 shows representative curves from one simple and one complex cell with effective mask contrasts ranging from 0 to 20%. The number of useful data points are sparse at higher mask contrasts; strong suppression eliminates responses at low base contrasts. Despite this problem, the change in the contrast-response function resulting from suppression appears to be either a rightward or downward shift rather than a slope change, indicating a change in contrast gain by a divisive mechanism. First-order regression lines were fitted to the response *versus* log contrast functions, omitting data points near the maintained discharge or saturation levels. The simple cell of Fig. 7A showed a range of log slope for all three curves spanning only 0.06, with no consistent trend for increase or decrease as mask contrast was increased. Contrast threshold (defined by intersection of the regression line with the resting discharge) was elevated 0.89 log units for a 20% mask. The complex cell showed slopes spanning 0.11 log units with contrast threshold elevation of 0.77 log units. As a figure of merit, the ratio of the change in log contrast threshold to the change in log slope was calculated for similar measurements made on a total of six cells and averaged 6.68, ranging from 3.55–14. The tendency of the mask to displace the response *versus* log contrast function without significant slope reduction seems clear, but this result is in conflict with that of Morrone et al. (1982), who report a slope reduction under similar circumstances. Regression lines fitted to the data from their Fig. 5 do show a change in threshold of 0.19 log unit for a noise mask

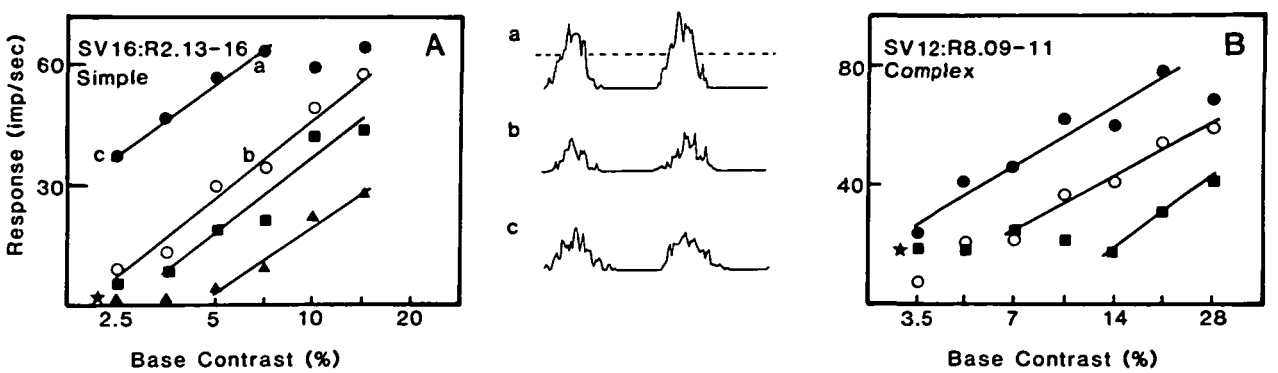

Fig. 7. Impact of inhibition on the response *versus* log contrast function of the recorded cell. Mask grating is oriented to provide inhibition, as in last figure. Star is maintained discharge. A, Simple cell. Mask contrasts of 0% (filled circles), 5% (open circles), 10% (squares), and 20% (triangles). Regression lines are analytically fit, omitting points near threshold or saturation. Raw responses from labeled data points show that response reduction due to inhibition is not quite an "iceberg" effect due to threshold elevation. The dotted line cutting response "a" yields a waveform that is of equal amplitude but temporally narrower than the inhibited response (b), which is closer in width to a response produced with lower contrast (c). Spatial frequency, 0.7 cycles/deg. B, Similar manipulation for a complex cell. Symbols for mask contrast as in A. Spatial frequency, 0.6 cycles/deg.

of 37% contrast, but the slope change is larger at 0.29 log unit. I have no explanation for this discrepancy.

Discrimination between a downward or rightward shift of response *versus* log contrast curves would be possible if saturation were evident, but saturation is minimal due to the limited contrast range of each of the two gratings. A downward shift represents simple algebraic subtraction and could result from steady hyperpolarization of the cell by nonoptimal stimulation, as described by Creutzfeldt et al. (1974*b*). Response amplitude would be decreased by an "iceberg" effect, in which only the response peaks are suprathreshold. This is not exactly the case here, since examination of the response histograms (center, Fig. 7) reveals that the temporal width of each phase of the (synchronous, simple cell) response remains essentially unchanged with higher mask contrast (compare "b" with "a"), despite marked reduction of response amplitude. The form of the response resembles more closely that resulting from single grating stimulation with low contrasts (cf. "c"). The mechanism reducing the response therefore seems to emulate contrast attenuation, which would result from a rightward shift of the response *versus* log contrast function. A similar rightward shift is also clearly seen under conditions of contrast adaptation of cortical cells (Ohzawa et al., 1985). Contrast adaptation seems to follow a power law with an exponent of about 0.9 (calculated from Fig. 3 of Ohzawa et al.). Inhibition in the six neurones studied here followed a power law with an exponent averaging also about 0.9, but the range spanned from 0.69–1.26, so this figure may not be representative. The broad spatial selectivity of the primary suppressive mechanism reported here (also to be expanded upon below) coupled with its dynamic behavior suggests strongly that it is closely associated with the contrast-adaptation mechanism described by Ohzawa et al. (1985). It is worth noting that the nearly pure rightward shift seen here is complementary to the pure slope changes seen in the presence of excess acetylcholine (DeBruyn et al., 1986).

Temporal characteristics of suppression

The temporal bandpass of the response-suppression mechanism was measured by varying the temporal frequency of drift of the mask grating (Fig. 8A and B). Strong suppression is found at lower temporal frequencies (up to 8 Hz), then decreases at 16 Hz. Masks drifting at 32 Hz have little impact on the response generated by the base. The reduced suppression seen at higher temporal frequencies reinforces the notion that it is mediated by cortical cells, which have a temporal-frequency bandpass in the cat of about 16 Hz (Movshon et al., 1978*c*) in contrast to the higher bandpass (40–60 Hz; Kaplan et al., 1979) of LGN cells.

When the mask orientation is varied, the d.c. response component demonstrates clear orientation selectivity for masks of 2 Hz and 3 Hz (filled symbols, Fig. 8C; similar measurements were demonstrated in Fig. 3). Elevation of the mask temporal frequency to 8 Hz, however, eliminates any component of orientation selectivity in the response (open circles, Fig. 8C); not only is the response flat over all orientations, it is also depressed below the control-response level. This is consistent with the interpretation of the results of harmonic decomposition of the response (e.g. Fig. 4). If we assume that the orientation-selective portion of the d.c. response is due primarily to excitation generated by the mask, it is unsurprising that this

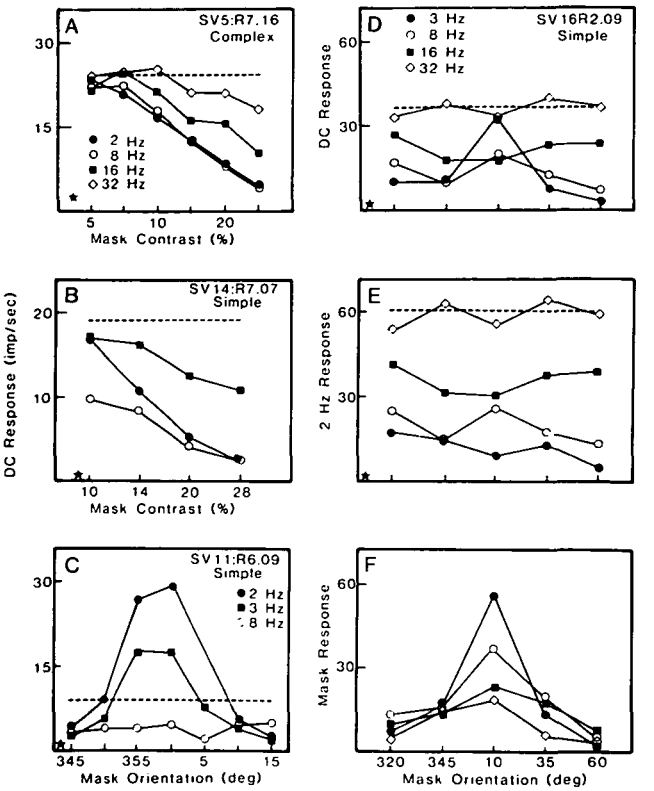

Fig. 8. Temporal-frequency characteristic of inhibition. Horizontal dotted line is response to base alone; star is maintained discharge. A, Mask is oriented to provide inhibition and drifted at frequencies of 2 Hz (filled circles), 8 Hz (open circles), 16 Hz (squares), and 32 Hz (diamonds). Inhibition is identical for 2 Hz and 8 Hz, but is reduced at 16 Hz, yet more at 32 Hz. Complex cell, spatial frequency 0.4 cycles/deg, b.e.c. 14%. B, Similar manipulation for a simple cell, symbols as above. Spatial frequency 0.4 cycles/deg, b.e.c. 7%. C, Orientation of mask is varied for temporal frequencies of 2 Hz (filled circles), 3 Hz (squares), and 8 Hz (open circles). The flatness of the 8-Hz curve is due to failure of that frequency to excite the cell; it is still effective at providing inhibition. Spatial frequency, 1.8 cycles/deg, b.e.c. 10%, m.e.c. 20%. D–F, Simple cell response decomposition for masks of different orientaiton and temporal frequency. Symbols as in A except 3 Hz (filled circles). D, d.c. response. E, 2-Hz (base) response shows poor orientation tuning of inhibition and organized reduction of inhibition as mask frequency is increased. F, 3-Hz (mask) response tuning is due to orientation-selective excitation, since peaks are absent in 2-Hz response. Peaks are reduced with increasing temporal frequency, as would be expected from the excitatory temporal bandpass of the recorded cell. Spatial frequency, 0.7 cycles/deg, b.e.c. 10%, m.e.c. 20%.

portion is nearly absent when the mask is drifted at 8 Hz, which is only weakly excitatory for most cortical cells. The 8-Hz mask does appear to cause suppression, since the d.c. response is well below the control-response level, and this suppression does not seem to be orientation selective, since the curve is flat across orientation. The effectiveness of suppression at 8 Hz implies that in this case the suppressive mechanisms have a somewhat higher temporal bandwidth than (and are therefore independent from) the cell under study.

Similar behavior was confirmed in another simple cell that allowed response decomposition (Fig. 8D–F). A mask was presented at five orientations and four temporal frequencies (3, 8, 16, and 32 Hz). Once again, the d.c. response (Fig. 8D) dem-

onstrates excitatory peaks at the optimal orientation for masks drifted at 3 Hz and, to a lesser extent, 8 Hz. A substantial response depression, with no apparent excitation, results from the 16-Hz mask (filled squares), while a 32-Hz mask (open diamonds) has no impact on the cell. The 2-Hz response component (Fig. 8E), in which the excitatory contributions of the mask are not present, shows monotonically decreasing suppression for masks of 3–16 Hz; the excitatory response induced by the mask (Fig. 8F) is, as expected, systematically reduced at higher temporal frequencies.

Spatial-frequency bandpass of suppression

The dependence of response suppression on spatial frequency was tested by situating the mask at an orientation that caused suppression and varying its spatial frequency. To facilitate comparison of the spatial-frequency bandpass of the suppressive mechanism with that of the recorded cell, in these figures the amount of suppression is shown by subtracting the actual response level from the half-contrast control level (i.e. what the response would be without the mask). The suppressed response is therefore expressed in negative impulses/s (indicating the response decrease below the control level; left ordinates, Fig. 9) while the excitatory spatial-frequency bandpass is expressed in the usual way (right ordinates). All of the 17 cells studied this way showed suppression that was effective over a much broader range of spatial frequencies (nearly a decade) than the excitatory bandwidth of the recorded cell and cortical cells in general, which have a bandwidth averaging 1.8 octaves (e.g. Movshon et al. 1978*c*). The complex cell of Fig. 9A has an excitatory peak at about 1.1 cycle/deg and a bandwidth of less than two octaves. The bandpass of suppression generated by a nonoptimally oriented mask has a very different appearance, with a broad peak at 0.5–0.8 cycles/deg and a range from below 0.2 to about 2 cycles/deg. For the simple cell shown in Fig. 9B, the 0.4 cycle/deg excitatory peak lies somewhat below the peak of the suppressive mechanism, again broadly falling between 0.5–0.8 cycles/deg. This cell allowed response decomposition, and showed a complementary relationship between the increase of suppression (in the 2-Hz response component) and the fall of excitation (3-Hz component) as mask spatial frequency increases from 0.2–0.8 cycles/deg. At spatial frequencies above 1.1, suppression is reduced (as seen in the drop of the 2-Hz curve) so that a small excitatory (3-Hz) component once again appears, even though it is attenuated by the limits of the excitatory bandpass. The dependence of the spatial-frequency tuning of the suppressive mechanism on mask contrast is shown in Fig. 9C. The relatively narrow bandpass

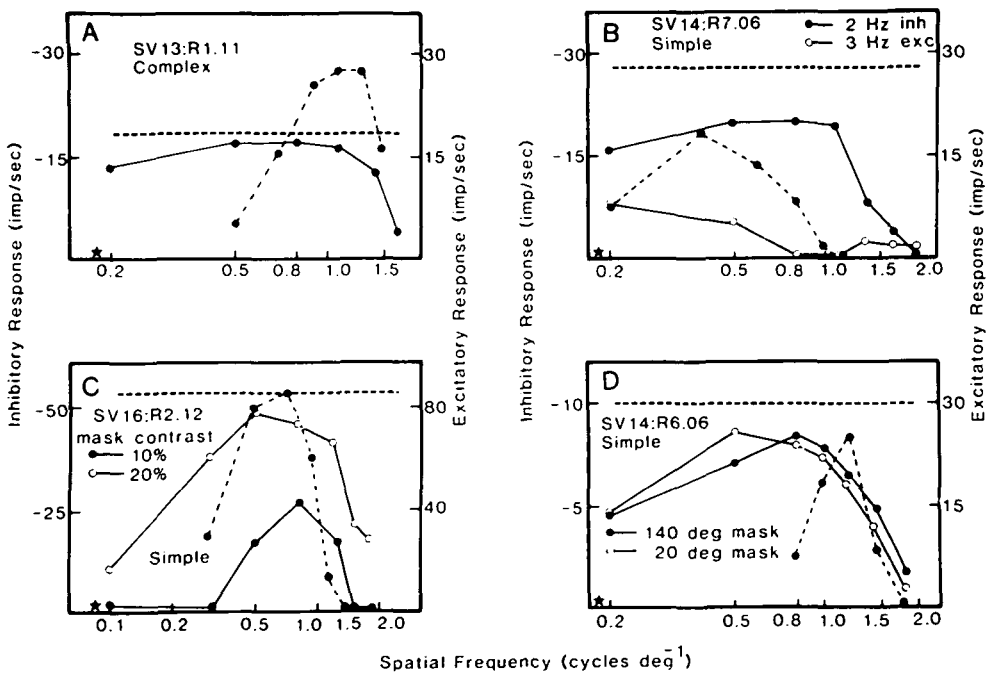

Fig. 9. Dependence of inhibition on spatial frequency. The excitatory spatial-frequency tuning functions, measured in the usual way, are represented by dotted curves (filled circles) and are associated with the positive ordinates on the right. A mask grating was then added and was oriented to suppress responses. The inhibitory response (solid curves) was calculated by subtracting the cell's actual response from the control level (horizontal dotted line), and is associated with the left-hand ordinates expressing negative impulses/s. This manipulation permits a more direct comparison of the bandpass of each mechanism. A, Typically broad inhibitory bandpass. Complex cell, base spatial frequency 1.1 cycles/deg, b.e.c. 14%, m.e.c. 20%. B (upper right), Simple cell response decomposition. Inhibition, as seen in the 2-Hz component (filled circles), is plotted inverted while excitation in the 3-Hz component (open circles) is plotted normally. The peak of inhibition at 0.8–1.0 cycles/deg eliminates the excitatory response in the same range. Base s.f. 0.4 cycles/deg, b.e.c. 7%, m.e.c. 20%. C (lower left), Suppression bandpass for simple cell at different mask contrasts; m.e.c. of 10% (filled circles) and 20% (open circles). Base spatial frequency 0.7 cycles/deg, b.e.c. 10%. D, Spatial-frequency bandpass of inhibition for two mask orientations, 20 deg (open circles) and 140 deg (filled circles), corresponding to limits of the excitatory tuning function. The small differences were consistent in this cell and resembled similar patterns in other cells. Base s.f. 1.2 cycles/deg, b.e.c. 14%, m.e.c. 28%.

resulting from a mask of 10% contrast is nearly doubled by a contrast increase to 20%. The increase in contrast also shifts the peak from about 0.8–0.5 cycles/deg; such shifts with contrast are not characteristic of excitatory tuning functions (Tolhurst & Movshon, 1975), implying that higher contrast may recruit contributions from suppressive mechanisms with a somewhat different spectral characteristic.

The shape of the inhibitory spatial-frequency tuning function also varied somewhat with mask orientation. Figure 9D shows inhibitory spatial-frequency tuning measured at two different mask orientations just at the limits (on either side) of the excitatory orientation-tuning function. Once again, the bandwidth is quite broad and the shape very different from the spatial-frequency tuning of the recorded cell. The differences between the two curves are small but consistent. Inhibition from one orientation (20 deg) is stronger at low spatial frequencies, and that from the other orientation (140 deg) is stronger at high spatial frequencies. Most of the cells studied this way had broad excitatory orientation tuning and suppression that was fairly uniform over orientation. The close similarity of the spatial-frequency tuning of suppression at different orientations and across cells is presumably another indicator of the very general organization of the pool of signals that is integrated to cause the suppression.

Discussion

Superimposition of a mask grating onto a base grating clearly has a major influence on the base-evoked responses of cortical cells but there may be some question as to the origins of this influence. A mask grating of appropriate orientation can, in many cells, eliminate entirely the response induced by the base grating. The mechanism supporting response reduction is not simply a decrease in excitation as a result of physical interference between the two gratings; while interference patterns are unavoidable, in these experiments the presence of contrast nulls over the receptive fields is time-averaged. Moreover, response reduction is graded, and responses *decrease* monotonically with *increasing* mask contrast. If response reduction were solely a result of contrast cancellation between gratings (as a result of grating segments being 180 deg out of phase), the reduction would be greatest when the contrasts of base and mask were identical. The small influence of the mask on the responses of all LGN cells (Fig. 2) and some cortical cells (Fig. 5B) indicates both that the site of response reduction is cortical and that physical interference is not a major cause of response reduction. Except in special cases, the response reduction is not a consequence of response compression or saturation in the recorded cell, since the response is usually low or absent when the reduction is greatest. It is therefore reasonable to conclude that the response reduction observed results from intracortical synaptic inhibition induced by the mask.

This finding is fundamentally in accord with results from other double-stimulus and pharmacological studies (e.g. Morrone et al., 1982; Sillito, 1979). However, most of these earlier studies were qualitative in nature and were concerned primarily with demonstrating simply the existence of inhibition generated by a nonoptimally oriented stimulus. The present results differ from the anticipations of these studies in two important ways. First, the sensitivity and strength of the inhibitory mechanisms are found here to vary broadly between cells. Although there is some correlation between suppressive effectiveness and sharpness of tuning, it is by no means perfect; for example, sharply tuned simple cells as well as broadly tuned complex cells can show very weak suppression. This implies that synaptic inhibition alone is not sufficient to account for orientation selectivity, and that mechanisms may vary between cells. Second, at least in simple cells, the spatial characteristics of the suppressive mechanisms do not support the notion that synaptic inhibition must be orientation selective in a way that is complementary to the excitatory orientation-tuning function. The dominant component appears instead to be essentially uniform across orientation. Only sharply tuned cells show a consistent dependence of suppression on orientation, and this is limited to narrow regions near the limits of the excitatory tuning function. Neither of these observations is inconsistent with earlier work, but some explanations are in order.

Sillito tested the impact of inhibition on orientation selectivity by comparing the responses to high-contrast bars drifted across the receptive field at orthogonal orientations. Application of a GABA-blocking agent (some form of bicuculline) modified these responses; if responses at each orientation appeared to be roughly equal then orientation selectivity was judged to have been eliminated. Complex cells showed partial (48%) or complete (52%) abolition of orientation selectivity (Sillito, 1979); a total loss of orientation selectivity was described in all (of 13) simple cells studied (Sillito et al., 1980). A total loss was interpreted as indicating that in the "uninhibited" state excitation was not strongly orientation dependent, and therefore orientation selectivity resulted from orientation-dependent inhibition. His results imply that inhibition is both more ubiquitous and more orientation selective than reported here. Although application of bicuculline may result in the reduction of GABA-mediated inhibition, it may not be an effective tool for judging the *strength* of inhibition, especially when high-contrast bars are used for stimulation. Equal responses at orthogonal orientations do not necessarily imply that orientation selectivity is eliminated or that excitation does not itself have some degree of orientation selectivity. Responses in the presence of bicuculline are markedly elevated (scales of 100–200 impulses/s in Sillito et al., 1980) and differences in response amplitude indicating intrinsic orientation selectivity of excitation could be masked by response saturation. Additionally, there is some evidence that bicuculline has a lesser impact on orientation tuning than reported by Sillito, at least when gratings are used for test stimuli (Pfleger et al., 1987).

Origins of the inhibition

There are many reasons to believe that the inhibition seen here is intracortical and stems from complex cells, as suggested by others (e.g. Creutzfeldt et al., 1974*a*; Lennie, 1980; Morrone et al., 1982; DeValois & Tootell, 1983). Although direct inhibition from LGN cells is an attractive theory in view of the non-oriented inhibitory behavior reported above, it is rejected in part because the high temporal bandwidth of LGN cells is not reflected in the relatively low bandwidth (16 Hz) of the inhibition, which is still somewhat higher than that of most simple cells. Moreover, both anatomical (Garey & Powell, 1971) and physiological (Creutzfeldt & Ito, 1968; Tanaka, 1985) evidence suggests that LGN afferents to cortex are purely excitatory. When mask gratings were positioned to evoke suppression but no excitation, no response component at the frequency of mask drift was ever seen. Modulation at the mask drift frequency

might be expected if the inhibition originated in a population of spatially linear simple cells. In addition, Morrone et al. (1982) found that the inhibition results in frequency doubling to flashed stimuli, a property of complex cells. The broadly selective spatial properties of the inhibition are also suggestive of complex cells, which tend to be more broadly tuned than simple cells in the domains of orientation and spatial frequency (Orban, 1984).

Unfortunately, there is no evidence for a physiological substrate to support this contention. Inhibition is believed to come primarily from smooth stellate cells, which have synapses that are likely to be inhibitory (LeVay, 1973; Peters & Fairen, 1978). They are distributed throughout all layers of the visual cortex and synapse with all other morphologic cell types, including themselves (Garey, 1971; Peters & Fairen, 1978). Furthermore, smooth stellate cells in the rat cortex contain glutamate decarboxylase, the enzyme responsible for the synthesis of GABA (Ribak, 1978). Functional characterization of identified smooth stellate cells suggests, however, that they are simple (Gilbert & Wiesel, 1979). Assessment of intracortical connectivity through cross correlation indicates that inhibition has thus far been found to originate in simple cell types with impact on both simple and complex cells, but there is no direct evidence for inhibition by any complex cells (Toyama et al., 1981). Given these constraints, the most likely source for the inhibition observed here is a large pool of simple cells, organized in a spatially incoherent manner. The large size of the pool is required because it must respond to essentially every spatial frequency and orientation to which the cat is sensitive; this broad sample contributes in turn to the lack of spatial linearity.

Inhibitory role in orientation selectivity

The orientation selectivity typical of cortical cells can be supported by a spatially general inhibitory pool if a cell receives excitation that has some innate bias for stimulus orientation. Tuned excitation arises naturally for cells receiving exclusively intracortical excitation, but the origin of tuned excitation for cells monosynaptically excited by the LGN is not yet clear, even though its existence is clear (Ferster, 1986). Retinal ganglion cells have shown some response dependence on orientation (e.g. Levick & Thibos, 1982). LGN cells have shown response ratios for orthogonal gratings averaging 2:1 (ranging to 7:1) in one study (Vidyasagar & Urbas, 1982) and 1.3:1 (ranging to 3:1) in another (Soodak et al., 1987). Even though excitatory response fields appear to be roughly radially symmetric (Creutzfeldt et al., 1974*b*; Heggelund, 1981*a*,*b*), in some fields there is a tendency for elongation. Gilbert and Wiesel (1983) note that the anatomy of cells in layer 6 provides a reasonable basis for synthesis of long fields.

Once orientation-biased excitation is assumed, the refinement of orientation selectivity appears to proceed in one or two stages. The most dominant mechanism is a floating threshold nonlinearity mediated by the inhibitory pool described above. This mechanism supports sensitivity to stimuli of low contrast while maintaining constant orientation-tuning bandwidths over a broad range of contrasts (Sclar & Freeman, 1982). Weak tonic suppression of a cortical cell at rest truncates most or all of the maintained discharge as well as the weaker responses from low-contrast stimulation at the orthogonal orientation, but slightly stronger excitation from optimally oriented stimuli causes the cell to fire. An increase in stimulus contrast results in an increase in excitation from stimuli at nonoptimal orientations; however, firing remains suppressed by the concomitant increase in inhibition. It is worth reiterating that this scheme does not specifically require inhibition from cells that are tuned to the orthogonal orientation, which is not well-supported on anatomical grounds (Gilbert & Wiesel, 1983). The scheme is consistent with the improvement of tuning seen with increased slit length. A longer slit would provide more contrast energy resulting in more inhibition, elevating threshold regardless of slit orientation and thereby narrowing the tuning curve.

At least in some simple cells, the floating-threshold mechanism is augmented by true orientation-selective inhibition. This latter mechanism may be a by-product of the architecture of area 17. Intracortical inhibition seems to be strongest when it arises from the same or neighboring orientation columns (Toyama et al., 1981). The locally selective inhibition seen here (e.g. Figs. 4D, 5C and D) seems to peak from 15–30 deg to each side of the optimal orientation. Orientation columns in the cat show a change in orientation of about 10 deg for every 50 μm of lateral distance (e.g. Albus, 1975). Most cortical cells that are filled with horseradish peroxidase show both local and widespread intrinsic connections, with the local projections appearing considerably more dense than the widespread processes (Gilbert & Wiesel, 1979, 1983). The majority of the local connections are located within about 150 μm of the soma when measured in a plane parallel to the cortical surface; stronger inhibition from neighboring (rather than orthogonal) orientations is thus not unexpected.

The existence of a local mechanism specifically intended to steepen the slopes of an orientation-tuning function, thereby increasing the orientation discriminability of a cell, is compatible with the general principles of organization of sensory systems. Lateral inhibition in the spatial domain, represented by Mach bands, results from a nerve network that is mutually and recurrently inhibitory (Ratliffe, 1965), and is fundamental to enhancing contrast discriminability and spatial-frequency selectivity. By plotting orientation on a linear abscissa, as in Fig. 5C, the parallel between local orientation-selective inhibitory peaks and spatial Mach bands is readily apparent, and the columnar organization of orientation selectivity in the cortex provides an appropriate anatomical analog to the organization of spatial lateral inhibition.

Unification of inhibitory influences

An inhibitory pool that is responsive to virtually any contrast to which the visual system can respond does not make much immediate sense as a mechanism solely intended to support orientation selectivity. However, inhibition is highly integrated into the function of the visual cortex, and it may be presumptuous to assign a single role to a mechanism that is so broadly influential. Excitatory postsynaptic potentials are invariably followed by inhibitory potentials delayed by one or more synapses (Creutzfeldt & Ito, 1968; Ferster & Lindstrom, 1983). Response saturation and the absence of a maintained discharge are commonly attributed to inhibition (Li & Creutzfeldt, 1984; Movshon et al., 1978*a*). Spatial adaptation in the visual cortex (Movshon & Lennie, 1979; Albrecht et al., 1984) may also depend on inhibition (Dealy & Tolhurst, 1974). Cortical cells are able to adjust their gain dynamically to keep their response at a usable level over a widely varying range of ambient contrasts (Ohzawa et al., 1985), and inhibition has been cited as a

source for this behavior although this inhibition is not likely to be GABA-mediated (DeBruyn & Bonds, 1986). All of these properties seem somehow to be linked, hence, it is not unreasonable to consider that they all—including the global inhibition reported here, that appears to enhance spatial selectivity—share the same physiological mechanism. Global inhibition and the cortical gain control share at least two characteristics: there appears to be a broad variation of the strength of these mechanisms from cell to cell, and both cause a pure rightward shift of the response *versus* log contrast function. There is also some evidence that the broad spatial selectivity of global inhibition is shared by the cortical contrast gain control, in that stimuli that do not excite a cell have impact on its gain (Ohzawa et al., 1985). The enhanced spatial selectivity of cortical cells may therefore prove to be an epi-phenomenon of a mechanism that has the rather broader charge of maximizing sensitivity to incremental changes in contrast.

The broadly selective spatial properties of the inhibitory pool suggests essentially complete communication between cortical cells serving a given region of the visual field. Mutual inhibition across spatial channels (e.g. lateral inhibition) is historically recognized as being advantageous for discrimination. It could also offer a significant advantage to the task of pattern recognition. In the cortex, the image in the visual field is transformed into a vector of very large dimension, in which each coefficient represents the firing rate of a given cortical cell. The firing rate is in turn a function of the amount of relative contrast over a limited range of spatial frequency, orientation, and location in the visual field. Such a coding scheme has been shown empirically to be highly efficient in representing images, at least for the human visual system (Watson, 1987). Recognition of an object could occur by matching of this vector with a template by associative memory mechanisms. Intracortical inhibition of the type described here has the potential to constrain the vector to unit (or constant) length, regardless of viewing conditions. This would reduce the properties of the vector to just a direction, which has the potential to simplify significantly the recognition process.

The body of evidence that is presented here supports a parallel system of information processing in the primary visual cortex that is divided into excitatory and inhibitory streams. The broad spatial definition of inhibition is uncharacteristic of the behavior of single cells, suggesting that the inhibitory network need not be dependent on the excitatory network. Because of its broad selectivity, the inhibitory network may serve many of the properties associated with cortical cells, although this does not rule out local inhibitory interactions serving specific purposes, e.g. fine tuning of orientation selectivity. The dynamic nature of the inhibitory network underscores the necessity to abandon the concept of the cortical neuron as a *single* unit with discrete and static receptive-field organization.

Acknowledgments

Ed DeBruyn helped to conduct these experiments. Shaul Hochstein and Robert Shapley provided stimulating discussion. The importance of global inhibition to pattern recognition was suggested by John Robson. Flaxedil was provided by the David & Geck division of American Cyanamid. This work was supported primarily by the National Eye Institute (Grant EY03778) with auxiliary help from the Vanderbilt University Research Council.

References

Albus, K. (1975). A quantitative study of the projection area of the central and paracentral visual field in the cat: the spatial organization in the orientation domain. *Experimental Brain Research* **24**, 181-202.

Albrecht, D.G., Farrar, S. & Hamilton, D.B. (1984). Spatial contrast adaptation characteristics of neurones recorded in the cat's visual cortex. *Journal of Physiology* **347**, 713-739.

Bishop, P.O., Coombs, J.S. & Henry, G.H. (1973). Receptive fields of simple cells in the cat striate cortex. *Journal of Physiology* **231**, 31-60.

Creutzfeldt, O.D. & Ito, M. (1968). Functional synaptic organization of primary visual cortex neurons in the cat. *Experimental Brain Research* **6**, 324-352.

Creutzfeldt, O.D., Innocenti, G.M. & Brooks, D. (1974*a*). Vertical organization in the visual cortex (Area 17). *Experimental Brain Research* **21**, 315-336.

Creutzfeldt, O.D., Kuhnt, U. & Benevento, L.A. (1974*b*). An intracellular analysis of visual cortical neurons to moving stimuli: responses in a cooperative neuronal network. *Experimental Brain Research* **21**, 251-274.

Dealy, R.S. & Tolhurst, D.J. (1974). Is spatial adaptation an aftereffect of prolonged inhibition? *Journal of Physiology* **241**, 261-270.

DeBruyn, E.J. & Bonds, A.B. (1986). Contrast adaptation in cat visual cortex is not mediated by GABA. *Brain Research* **383**, 339-342.

DeBruyn, E.J., Gajewski, Y.A. & Bonds, A.B. (1986). Anti-cholinesterase agents affect the gain of the cat cortical VEP. *Neuroscience Letters* 71, 311-317.

DeValois, K.K. & Tootell, R.B.H. (1983). Spatial-frequency-specific inhibition in cat striate cortex cells. *Journal of Physiology* **336**, 359-376.

Ferster, D. (1986). Orientation selectivity of synaptic potentials in neurons of cat primary visual cortex. *Journal of Neuroscience* **6**, 1284-1301.

Ferster, D. & Lindstrom, S. (1983). An intracellular analysis of geniculo-cortical connectivity in area 17 of the cat. *Journal of Physiology* **342**, 181-215.

Garey, L.J. (1971). A light and electron microscopic study of the visual cortex of the cat and monkey. *Proceedings of the Royal Society B* (London) **179**, 21-40.

Garey, L.J. & Powell, T.P.S. (1971). An experimental study of the termination of the lateral geniculo-cortical pathway in the cat. *Proceedings of the Royal Society B* (London) **179**, 41-63.

Gilbert, C.D. & Wiesel, T.N. (1979). Morphology and intracortical projections of functionally characterized neurones in the cat visual cortex. *Nature* **280**, 120-125.

Gilbert, C.D. & Wiesel, T.N. (1983). Clustered intrinsic connections in cat visual cortex. *Journal of Neuroscience* **3**, 1116-1133.

Hammond, P. (1978). On the use of nitrous oxide/oxygen mixtures for anesthesia in cats. *Journal of Physiology* **275**, 64P.

Heggelund, P. (1981*a*). Receptive-field organization of simple cells in cat striate cortex. *Experimental Brain Research* **42**, 89-98.

Heggelund, P. (1981*b*). Receptive-field organization of complex cells in cat striate cortex. *Experimental Brain Research* **42**, 99-107.

Henry, G.H., Bishop, P.O., Tupper, R.M. & Dreher, B. (1973). Orientation specificity of cells in cat striate cortex. *Vision Research* **13**, 1771-1779.

Hubel, D.H. & Wiesel, T.N. (1962). Receptive fields, binocular interaction, and functional architecture in the cat's visual cortex. *Journal of Physiology* **160**, 106-154.

Kaplan, E., Marcus, S. & So, Y.T. (1979). Effects of dark adaptation on spatial and temporal properties of receptive fields in cat lateral geniculate nucleus. *Journal of Physiology* **294**, 561-580.

Legge, G.E. & Foley, J.M. (1980). Contrast matching in human vision. *Journal of the Optical Society of America* **70**, 1458-1471.

Lennie, P. (1980). Parallel visual pathways: a review. *Vision Research* **20**, 561-594.

LeVay, S. (1973). Synaptic patterns in the visual cortex of the cat and monkey. Electron microscopy of Golgi preparations. *Journal of Comparative Neurology* **150**, 53-86.

Levick, W.R. (1972). Another tungsten microelectrode. *Medical and Biological Engineering* **10**, 510-515.

LEVICK, W.R. & THIBOS, L.N. (1982). Analysis of orientation bias in cat retina. *Journal of Physiology* **329**, 243–261.

LI, C.Y. & CREUTZFELDT, O.D. (1984). The representation of contrast and other stimulus parameters by single neurons in area 17 of the cat. *Pflugers Archives* **401**, 304–314.

MILKMAN, N., SHAPLEY, R.M. & SCHICK, G. (1978). A microcomputer-based visual stimulator. *Behavior Research Methods and Instrumentation* **10**, 539–545.

MORRONE, M.C., BURR, D.C. & MAFFEI, L. (1982). Functional implications of cross-orientation inhibition of cortical visual cells. *Proceedings of the Royal Society of London (Biology)* **216**, 335–354.

MOVSHON, J.A. & LENNIE, P. (1979). Pattern-selective adaptation in visual cortical neurones. *Nature* **278**, 850–851.

MOVSHON, J.A., THOMPSON, I.D. & TOLHURST, D.J. (1978*a*). Spatial summation in the receptive fields of simple cells in the cat's striate cortex. *Journal of Physiology* **283**, 53–77.

MOVSHON, J.A., THOMPSON, I.D. & TOLHURST, D.J. (1978*b*). Receptive field organization of complex cells in the cat's striate cortex. *Journal of Physiology* **283**, 79–99.

MOVSHON, J.A., THOMPSON, I.D. & TOLHURST, D.J. (1978*c*). Spatial and temporal contrast sensitivity of neurones in areas 17 and 18 of the cat's visual cortex. *Journal of Physiology* **283**, 101–120.

NELSON, J.I. & FROST, B.J. (1978). Orientation-selective inhibition from beyond the classic visual receptive field. *Brain Research* **139**, 359–364.

OHZAWA, I., SCLAR, G. & FREEMAN, R.D. (1985). Contrast gain control in the cat visual system. *Journal of Neurophysiology* **54**, 651–665.

ORBAN, G.A. (1984). *Neuronal Operations in the Visual Cortex*. Berlin: Springer-Verlag.

PETERS, A. & FAIREN, A. (1978). Smooth and sparsely spined stellate cells in the visual cortex of the rat: a study using a combined Golgi-electron microscope technique. *Journal of Comparative Neurology* **181**, 129–172.

PFLEGER, B., BONDS, A.B. & DEBRUYN, E.J. (1987). The limited role of GABA in orientation tuning of visual cortical cells of the cat. *Investigative Ophthalmology and Visual Science* (Suppl.) **28**, 198.

RATLIFFE, F. (1965). *Mach Bands: Quantitative Studies on Neural Networks in the Retina*. San Francisco: Holden-Day.

RIBAK, C.E. (1978). Aspinous and sparsely spinous stellate neurons in the visual cortex of rats contain glutamic acid decarboxylase. *Journal of Neurocytology* **7**, 461–478.

SCLAR, G. & FREEMAN, R.D. (1982). Orientation selectivity in the cat's striate cortex is invariant with stimulus contrast. *Experimental Brain Research* **46**, 457–461.

SILLITO, A.M. (1975). The contribution of inhibitory mechanisms to the receptive-field properties of neurones in the striate cortex of the cat. *Journal of Physiology* **250**, 305–329.

SILLITO, A.M. (1977). Inhibitory processes underlying the directional specificity of simple, complex, and hypercomplex cells in the cat's visual cortex. *Journal of Physiology* **271**, 699–720.

SILLITO, A.M. (1979). Inhibitory mechanisms influencing complex cell orientation selectivity and their modification at high resting discharge levels. *Journal of Physiology* **289**, 33–53.

SILLITO, A.M., KEMP, J.A., MILSON, J.A. & BERARDI, N. (1980). A reevaluation of the mechanisms underlying simple cell orientation selectivity. *Brain Research* **194**, 517–520.

SOODAK, R.E., SHAPLEY, R.M. & KAPLAN, E. (1987). Linear mechanism of orientation tuning in the retina and lateral geniculate of the cat. *Journal of Neurophysiology* **58**, 267–275.

TANAKA, K. (1985). Organization of geniculate inputs to visual cortical cells in the cat. *Vision Research* **25**, 357–364.

TOLHURST, D.J. & MOVSHON, J.A. (1975). Spatial and temporal contrast sensitivity of striate cortical neurones. *Nature* **257**, 674–675.

TOYAMA, K., KIMURA, M. & TANAKA, K. (1981). Cross-correlation analysis of interneural connectivity in cat visual cortex. *Journal of Neurophysiology* **46**, 191–201.

TSUMOTO, T., ECKART, W. & CREUTZFELDT, O.D. (1979). Modification of orientation sensitivity of cat visual cortex neurons by removal of GABA-mediated inhibition. *Experimental Brain Research* **34**, 351–363.

VIDYASAGAR, T.R. & URBAS, J.V. (1982). Orientation sensitivity of cat LGN neurones with and without inputs from visual cortical areas 17 and 18. *Experimental Brain Research* **46**, 157–169.

WATSON, A.B. (1987). Efficiency of human visual image codes. *Investigative Ophthalmology and Visual Science* (Suppl.) **28**, 365.